Therapeutic Radiometals Beyond ^{177}Lu and ^{90}Y: Production and Application of Promising α-Particle, β$^-$-Particle, and Auger Electron Emitters

Cristina Müller[1,2], Nicholas P. van der Meulen[1,3], Martina Benešová[1,2], and Roger Schibli[1,2]

[1]Center for Radiopharmaceutical Sciences ETH-PSI-USZ, Paul Scherrer Institut, Villigen-PSA, Switzerland; [2]Department of Chemistry and Applied Biosciences, ETH Zurich, Zurich, Switzerland; and [3]Laboratory of Radiochemistry, Paul Scherrer Institut, Villigen-PSA, Switzerland

In recent years, new α-particle–, β$^-$-particle–, and Auger electron–emitting radiometals—such as ^{67}Cu, ^{47}Sc, ^{166}Ho, ^{161}Tb, ^{149}Tb, ^{212}Pb/^{212}Bi, ^{225}Ac, and ^{213}Bi—have been produced and evaluated (pre)clinically for therapeutic purposes. In this short review article, the most important routes of production of these radiometals are critically discussed, as are examples of their application in preclinical and clinical studies.

Key Words: radiometals; α-particles; β$^-$-particles; Auger electrons; radionuclide therapy

J Nucl Med 2017; 58:91S–96S
DOI: 10.2967/jnumed.116.186825

Radionuclide tumor therapy has been used successfully for the treatment of disseminated disease (*1*). However, clinical application of therapeutic radionuclides is often driven by the availability of radionuclides rather than appropriate decay characteristics for a given disease indication. ^{90}Y and ^{177}Lu are routinely used for targeted radionuclide therapy (*1*). ^{90}Y decays with a shorter half-life ($t_{1/2}$) than ^{177}Lu.

The emission of high-energy β$^-$-particles has been used for radionuclide therapy in combination with peptides (e.g., ^{90}Y-DOTATOC) and antibodies (e.g., ibritumomab tiuxetan [Zevalin; Spectrum Pharmaceuticals, Inc.]) (*1*). ^{177}Lu emits low-energy β$^-$-particles as well as γ-radiation, useful for dosimetry (Table 1) (*1*). It has been used for peptide receptor–targeted radionuclide therapy (*2*) and in combination with small molecules, such as prostate-specific membrane antigen (PSMA) ligands (*3*). Because of the relatively long range of β$^-$-particles in tissue, tumor cells that are not directly targeted may also be affected. This so-called "crossfire" effect renders β$^-$-emitters more suited for the therapy of larger metastases (*4*).

In contrast to the low linear energy transfer (LET; ~0.2 keV/mm) of β$^-$-particles, α-particles have a high LET (80–100 keV/μm) but a shorter tissue range (*4*). The promising potential of high-LET radionuclides was demonstrated recently using $^{223}RaCl_2$ (Xofigo; Bayer), which revived interest in α-emitters (*5*). Auger electrons induce multiple ionizations (LET, 4–26 keV/μm) in the immediate vicinity of the decay site and, thus, are promising for the treatment of single cancer cells (*4*).

In the introduction of new radionuclides for therapy, several properties should be taken into consideration. For the treatment of disseminated disease, the emission of high-LET particles is of particular interest; the coemission of radiation (for PET or SPECT) that can be imaged or the existence of a readily available diagnostic match is clearly an advantage. Moreover, the chemical properties of the radiometal should allow stable coordination using standard chelators. The half-life of the radiometal should match the clinical indications and logistics. The method of production needs to be safe and affordable to allow continuous worldwide supply of the radionuclide at a high quality and in a sufficient quantity.

Here we discuss the therapeutic radionuclides ^{47}Sc, ^{67}Cu, ^{149}Tb, ^{161}Tb, ^{166}Ho, ^{212}Pb/^{212}Bi, ^{225}Ac, and ^{213}Bi (Table 1), selected in accordance with the aforementioned criteria.

COPPER-67

^{67}Cu is a low-energy β$^-$-emitter with γ-ray emission, useful for SPECT (Table 1). Studies using reactors and accelerators to produce ^{67}Cu have been performed (*6*). The ^{68}Zn(p,2p)^{67}Cu route of production (proton energy, >70 MeV) appears to be most attractive (*7*); however, besides the desired ^{67}Cu, large quantities of ^{64}Cu ($t_{1/2}$, 12.7 h) and ^{67}Ga ($t_{1/2}$, 78.3 h) are coproduced. The described separation methods required sizable columns containing chelating resin for primary separation to recover trace amounts of ^{67}Cu from gram quantities of Zn target material (*6,7*). At present, there is a shortage of ^{67}Cu supply, mainly because of the lack of cyclotrons producing high-energy protons.

Chelation of copper nuclides with a variety of macrocycles, including 1,4,7,10-tetraazacyclododecane-1,4,7,10-tetraacetic acid (DOTA), 1,4,8,11-tetraazacyclotetradecane-*N*,*N*′,*N*″,*N*‴-tetraacetic acid (TETA), 1,4,7-triazacyclononane-*N*-glutaric acid-*N*′,*N*″-diacetic acid (NODAGA), and 4-[(1,4,8,11-tetraazacyclotetradec-1-yl) methyl]benzoic acid (CPTA), as well as cross-bridged macrocycles (e.g., 1,4,8,11-tetraazabicyclo[6.6.2]hexadecane-4,11-diacetic acid [CB-TE2A]) and cage-type chelates (e.g., 1,8-diamino-3,6,10,13,16,19-hexaazabicyclo[6,6,6]-eicosane [DiAmSar]) (*8,9*), has been reported. Generally, the chelation of copper with tetraazamacrocycles results in low tumor-to-background ratios because of the transchelation of copper to proteins accumulating in the liver (*8*). However, Zimmermann et al. (*10*) and Grünberg et al. (*11*) reported

Received Feb. 7, 2017; revision accepted Mar. 13, 2017.
For correspondence or reprints contact: Roger Schibli, Center for Radiopharmaceutical Sciences ETH-PSI-USZ, Paul Scherrer Institut, 5232 Villigen, Switzerland.
E-mail: roger.schibli@psi.ch

TABLE 1
Decay Characteristics, Production Routes, and Diagnostic Matches for Radiometals for Therapeutic Application

Radionuclide	Half-life	Eα (keV)*	$Eβ^-_{average}$ (keV)	Eγ or $Eβ^+$ (keV)*	Production method	Chelator	Diagnostic match
^{90}Y	2.67 d		934		^{90}Sr/^{90}Y generator ^{90}Zr(n,p)^{90}Y ^{89}Y(n,γ)^{90}Y	DTPA (tiuxetan), DOTA	
^{177}Lu	6.65 d		134	γ: 113 (6.2)† γ: 208 (10.4)†	^{176}Lu(n,γ)^{177}Lu (*74*) ^{176}Yb(n,γ)^{177}Yb → ^{177}Lu (*75*)	DOTA	
^{67}Cu	2.58 d		141	γ: 91 (7.0)† γ: 93 (16.1)† γ: 185 (48.7)†	^{68}Zn(p,2p)^{67}Cu (*7*) ^{68}Zn(γ,p)^{67}Cu (*76*) ^{70}Zn(p,α)^{67}Cu (*77*) ^{70}Zn(d,αn)^{67}Cu (*78*)	NOTA, NODAGA, TETA, CPTA, (DOTA), cross-bridged macrocycles (*8*)	^{64}Cu (PET) ^{62}Cu (PET) ^{61}Cu (PET)
^{47}Sc	3.35 d		162	γ: 159 (68.3)†	^{47}Ti(n,p)^{47}Sc (*18,19*) ^{46}Ca(n,γ)^{47}Ca → ^{47}Sc (*17,19*) ^{48}Ca(γ,n)^{47}Ca → ^{47}Sc (*21*)	DOTA (*17*), AAZTA (*24*), DO3AP (*23*)	^{43}Sc (PET) ^{44}Sc (PET)
^{166}Ho	1.11 d		665	γ: 81 (6.6)† γ: 1,379 (0.9)	^{165}Ho(n,γ)^{166}Ho (*26*) ^{164}Dy(2n,γ)^{166}Dy → ^{166}Ho (*31*)	DOTA (*32*)	
^{161}Tb	6.89 d		154	γ: 49 (17.0)† γ: 75 (10.2)†	^{160}Gd(n,γ)^{161}Gd → ^{161}Tb (*35*)	DOTA (*37*)	^{152}Tb (PET) ^{155}Tb (SPECT)
^{149}Tb	4.118 h	3,967 (16.7)		β$^+$: 730 (7.1) γ: 165 (26.4)† γ: 352 (29.4) γ: 389 (18.4)	Nd(^{12}C,5n)^{149}Dy → ^{149}Tb (*42*) Spallation of tantalum target (*37,42*)	DOTA (*37*)	^{152}Tb (PET) ^{155}Tb (SPECT)
^{212}Pb (^{212}Bi)	10.64 h (60.6 min)	6,050 (25.1)‡ 6,089 (9.75)‡	100	γ: 238 (43.6) γ: 300 (3.3)‡	^{224}Ra/^{212}Pb generator (*48*)	DOTA (*48*), TCMC (*48*)	
^{225}Ac	10.0 d	5,637 (4.4) 5,732 (8.0) 5,791 (8.6) 5,793 (18.1) 5,830 (50.7)		γ: 99.8 (1.0)§	^{232}Th(p,2p6n)^{225}Ac (*55,56*) ^{226}Ra(p,2n)^{225}Ac (*57*) ^{226}Ra(γ,n)^{225}Ra → ^{225}Ac (*58*)	DOTA (*63*)	
^{213}Bi	45.6 min	5,558 (0.181) 5,875 (1.96)		γ: 324 (0.17)	^{225}Ac/^{213}Bi generator (*52*)	DOTA (*52*)	

*Values are given as keV (values in parentheses represent intensity I in %).
†γ-energies useful for scintigraphy or SPECT.
‡For ^{212}Bi.
§For imaging with γ-rays of ^{225}Ac daughter nuclides ^{213}Bi and ^{221}Fr (*68*).
DTPA = diethylenetriaminepentaacetic acid; AAZTA = 1,4-bis(carboxymethyl)-6-[bis(carboxymethyl)]amino-6-methylperhydro-1,4-diazepine; DO3AP = 1,4,7,10-tetraazacyclododecane-1,4,7-triacetic-10-methylphosphonic acid.

the successful use of DOTA and CPTA chelators in preclinical studies performed with a ^{67}Cu-labeled anti–L1-CAM antibody and F(ab′)$_2$ fragments.

In a pilot study, ^{67}Cu-labeled anti-MUC1 mucin antibody C595 was evaluated for targeting bladder cancer after intravesical administration into cystectomy specimens (*12*). A study was performed in non-Hodgkin lymphoma patients with ^{67}Cu-labeled TETA–Lym-1 antibody at diagnostic quantities followed by 4 therapy cycles (*13*). This radioimmunotherapy was revealed to be safe and effective (*14,15*). In 6 patients with colorectal tumors, ^{67}Cu-labeled CPTA-mAB35 used for imaging purposes before surgery revealed high tumor uptake and favorable tumor-to-blood ratios relative to the results obtained with ^{131}I-labeled antibody (*16*). These promising clinical results and the relatively easy access to ^{64}Cu as a diagnostic match warrant further efforts to fully assess the therapeutic potential of ^{67}Cu.

SCANDIUM-47

^{47}Sc has decay characteristics similar to those of ^{67}Cu and also has with ^{44}Sc its theranostic match for PET (Table 1) (*17*). ^{47}Sc can be produced with neutrons via the ^{47}Ti(n,p)^{47}Sc (*18,19*) or

$^{46}Ca(n,\gamma)^{47}Ca \rightarrow {}^{47}Sc$ (*19,20*) nuclear reaction. The production of ^{47}Ca via the $^{48}Ca(\gamma,n)^{47}Ca$ nuclear reaction with electron linear accelerators was also evaluated (*21*). The production of ^{47}Sc via $^{48}Ti(p,2n)^{47}Sc$ was attempted, but too much of the long-lived ^{46}Sc was coproduced (*19*). The calcium route is straightforward because easy separation and ingrowing product allow for repeated separations (generator principle) (*20*).

With regard to complex formation and stability, it was revealed that DOTA forms stable scandium complexes (*22*). Recently, more specific chelators for scandium, such as monophosphorus acid DOTA analogs and AAZTA, were developed (*23,24*). The therapeutic potential of ^{47}Sc was demonstrated with a DOTA-folate conjugate; reduced tumor growth and increased average survival time in mice were observed (*17*). Moreover, high-quality SPECT images were obtained in mice that received ^{47}Sc-DOTA-folate (*17*). On the basis of these data, ^{47}Sc seems to have promise for clinical application.

HOLMIUM-166

^{166}Ho, a high-energy β^--emitter similar to ^{188}Re ($E^{\beta-}$ average, 763 keV; $t_{1/2}$, 17.0 h), coemits γ-rays useful for SPECT (Table 1). ^{166}Ho is most frequently produced via the $^{165}Ho(n,\gamma)^{166}Ho$ route in combination with poly–lactic acid microspheres for intraarterial radioembolization in patients with liver metastases (*25*). For this purpose, ^{nat}Ho is incorporated into microspheres and activated with neutrons (*26*). ^{166}Ho-microspheres administered intraarterially accumulated about 6-fold more in the tumor than in normal liver tissue in rats (*27*). Toxicity studies revealed no clinically relevant side effects in pigs (*28*). A phase 1 trial of intraarterial radioembolization using ^{166}Ho-labeled poly–lactic acid microspheres was designed for the treatment of patients with liver cancer (*25*). ^{166}Ho-based microspheres are considered to be superior to ^{90}Y-based glass or resin microspheres because of the low cost of production of ^{166}Ho and the possibility of SPECT imaging preceding therapy (*26,29*). Moreover, because holmium is highly paramagnetic, it can be visualized using MRI (*25*).

Clinical studies were performed to determine the safety and efficacy of treatment of hepatocellular carcinoma with a percutaneously administered ^{166}Ho-chitosan complex (*30*). The ^{166}Ho-chitosan complex therapy was efficient in terms of response and survival, and toxicity was acceptable, especially in patients with smaller tumors (*30*).

^{166}Ho can also be produced via the $^{164}Dy(2n,\gamma)^{166}Dy \rightarrow {}^{166}Ho$ nuclear reaction, yielding a carrier-free product useful for labeling of biomolecules (*31*). Among several investigated chelators, DOTA was found to be favorable and the kinetics of distribution of ^{166}Ho-DOTA were similar to those of ^{177}Lu-DOTA (*32*). The clinical safety and efficacy of ^{166}Ho-labeled macrocyclic tetraphosphonate-1,4,7,10-tetraazacyclododecane-1,4,7,10-tetramethylene-phosphonic acid (DOTMP) were assessed for skeleton-targeted radiotherapy of breast cancer–related bone metastases (*33*). The median overall survival time was 39.9 mo, and 2 patients remained progression-free for more than 6 y (*33*). A multicenter dose escalation study demonstrated the potential of ^{166}Ho-DOTMP for the treatment of multiple myeloma (*34*).

TERBIUM-161

^{161}Tb has chemical and physical characteristics similar to those of ^{177}Lu but coemits a substantial number of Auger electrons in addition to β^--particles (*35,36*). ^{161}Tb can be produced at a high specific activity by irradiation of enriched ^{160}Gd in a reactor with a high neutron flux via the $^{160}Gd(n,\gamma)^{161}Gd \rightarrow {}^{161}Tb$ nuclear reaction (*35*). The separation of ^{161}Tb from the gadolinium target material was performed by cation-exchange chromatography with α-hydroxyisobutyric acid followed by concentration of the ^{161}Tb solution (*37*), similar to the production of ^{177}Lu. Müller et al. were the first to use ^{161}Tb in a preclinical therapy setting, with tumor-bearing mice (*37*). An improved therapeutic effect of ^{161}Tb compared with that of ^{177}Lu was described in 2 independent preclinical studies (*38–40*). The coemitted Auger electrons appeared to be favorable for therapeutic purposes, but the clinical superiority of ^{161}Tb over ^{177}Lu remains to be assessed when a steady supply of ^{161}Tb can be guaranteed.

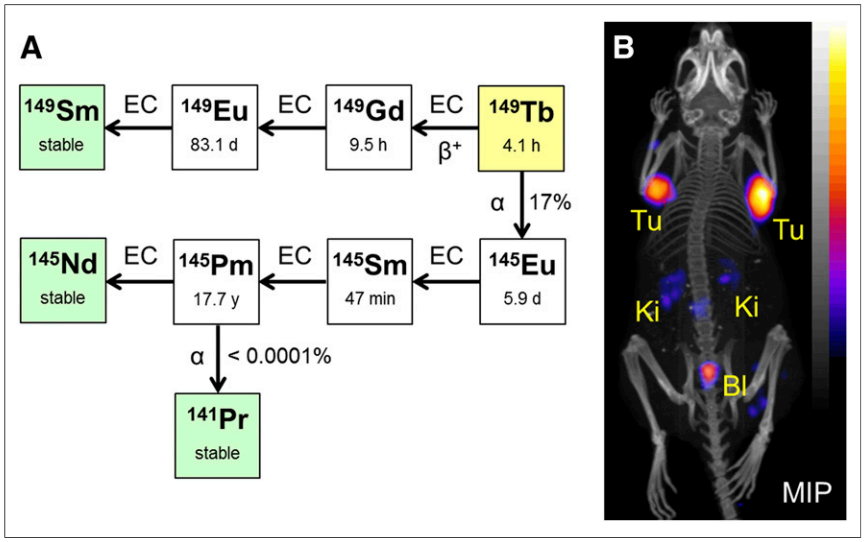

FIGURE 1. (A) Decay of ^{149}Tb to stable ^{149}Sm, ^{145}Nd, and ^{141}Pr. EC = electron capture. (B) Maximum-intensity projection (MIP) of PET/CT image of AR42J tumor–bearing mouse 2 h after injection of ^{149}Tb-DOTANOC (7 MBq). Bl = urinary bladder; Ki = kidney; Tu = tumor. (Adapted with permission of (*45*).)

TERBIUM-149

^{149}Tb was first proposed for targeted α-therapy by Allen and Blagojevic (*41*). Unlike most α-emitters, it decays predominantly by the emission of a single low-energy α-particle, positrons, and γ-radiation (Fig. 1A) (*42*). Beyer et al. chose the $Nd(^{12}C,5n)^{149}Dy \rightarrow {}^{149}Tb$ production route at the European Organization for Nuclear Research (*42*). Later, ^{149}Tb was produced by proton-induced spallation of a tantalum target followed by an online isotope separation process (*37,42,43*). In this scenario, ^{149}Tb had to be separated from isobars and pseudoisobars with a mass of 149 using cation-exchange chromatography (*37,42,43*).

The first preclinical therapy study with ^{149}Tb was performed in a mouse model of leukemia with ^{49}Tb-labeled cyclohexane-DTPA–functionalized rituximab (*43*). This therapy resulted in the long-term survival of mice without evidence of recurrence 120 d after

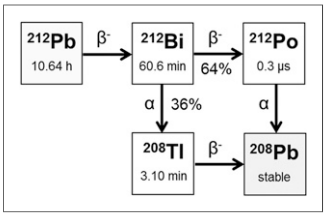

FIGURE 2. Decay of ^{212}Pb to ^{212}Bi and stable ^{208}Pb.

treatment, whereas untreated mice or mice treated with a high dose of rituximab reached endpoint criteria after 37 or 43 d, respectively (*43*). Müller et al. reported the potential of ^{149}Tb-DOTA-folate to treat KB tumor–bearing mice (*37,44*). The same group also investigated the positron emission of ^{149}Tb, potentially allowing PET simultaneously with α-therapy (Fig. 1B) (*45*).

LEAD-212 (AND BISMUTH 212)

The β^--emitter ^{212}Pb has been proposed as an in vivo α-emitter generator because of its α-emitting daughter nuclide, ^{212}Bi (Fig. 2). ^{203}Pb was recently described as a diagnostic match that can be readily produced from ^{nat}Tl via the ^{203}Tl(p,n)^{203}Pb nuclear reaction (*46*). The supply of ^{212}Pb is based on the availability of ^{228}Th extracted from spent nuclear fuel. Because ^{228}Th-based generators were affected by radiolytic damage, a generator based on ^{224}Ra ($t_{1/2}$, 3.66 d) was developed using ^{228}Th (*47*). The elution of ^{212}Pb from the ^{224}Ra/^{212}Pb generator requires several steps, including separation from the daughter nuclide, ^{212}Bi (*48*).

^{212}Pb can be coordinated using a DOTA chelator or *S*-2-(4-isothiocyanatobenzyl)-1,4,7,10-tetraaza-1,4,7,10-tetra(2-carbamoylmethyl) cyclododecane (TCMC), a macrocyclic chelator specifically developed for the complexation of lead (*48*). ^{212}Pb-labeled antibodies were investigated in several studies, including human epidermal growth factor 2 (HER2)–targeting trastuzumab in mouse models of peritoneal cancer or orthotopic models of prostate cancer (*48*). Two clinical studies performed in patients with HER2-positive cancer to determine the safety, distribution, and pharmacokinetics of ^{212}Pb-TCMC-trastuzumab and to determine dosimetry in a dose-escalation study indicated good tolerance and no evidence of radiation-related toxicity (*49,50*).

ACTINIUM-225

The decay of ^{225}Ac results in 6 daughters (^{221}Fr, ^{217}At, ^{213}Bi, ^{213}Po, ^{209}Pb, and ^{209}Bi) with several α- and β^--disintegrations (Fig. 3) (*51*). ^{213}Bi has been investigated extensively for α-therapy in (pre)clinical studies (*52*). ^{225}Ac can be obtained in limited quantities (~37 GBq/y) by radiochemical separation from a ^{229}Th source (*53,54*). It can also be produced via the ^{232}Th(p,2p6n)^{225}Ac (*55,56*), ^{226}Ra(p,2n)^{225}Ac (*57*), and ^{226}Ra(γ,n)^{225}Ra → ^{225}Ac nuclear reactions (*58*). The separation of ^{225}Ac from the ^{226}Ra target material was performed using lanthanide extraction resin chromatography (*53*). For the separation of ^{225}Ac from its target material, a cumbersome 5-column system was reported (*54*). Because any target material used is radioactive (and long-lived), additional safety precautions must be taken into consideration during production.

The use of ^{225}Ac may be challenging because of its decay chain and the fact that the first disintegration leads to the destruction of the metal complex (because of the high recoil energy) and the subsequent mobilization of the daughter radionuclides—a feature shared by all α-particle–emitting radionuclides (*59–61*).

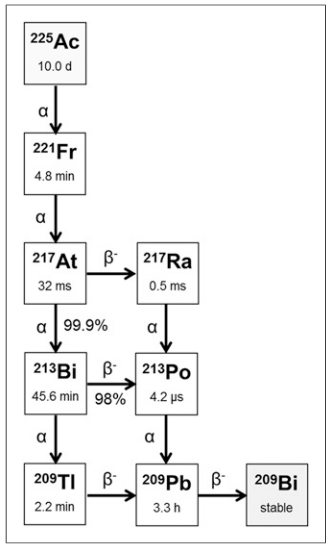

FIGURE 3. Decay of ^{225}Ac to ^{213}Bi and stable ^{209}Bi.

DOTA chelators have been used to conjugate ^{225}Ac to antibodies and small molecules (*62*). The effectiveness of ^{225}Ac-labeled antibodies (such as anti-CD33, anti-CD18, anti-HER2/neu, and anti-PSMA) was demonstrated in vitro against leukemia and lymphoma as well as breast, ovarian, and prostate cancer cells (*63*). The treatment of prostate tumor–bearing mice with the PSMA-specific antibody ^{225}Ac-J591 improved survival time over that of mice receiving unlabeled J591 (*63*). Other preclinical studies demonstrated the successful treatment of AR42J tumor–bearing mice with ^{225}Ac-DOTATOC (*64*) and dose-dependent antitumor effects after treatment with ^{225}Ac-labeled trastuzumab in an intraperitoneal ovarian tumor mouse model (*65*).

A phase 1 study with the anti-CD33 antibody ^{225}Ac-lintuzumab (HuM195) was performed in patients with relapsed/refractory acute myeloid leukemia (*66*). Across all dose levels, antileukemic activity was evident. No acute toxicity other than liver function abnormalities occurred (*66*). A multicenter phase 1 trial with ^{225}Ac-lintuzumab in combination with low-dose cytarabine resulted in a remarkable response represented by bone marrow blast reduction in more than 50% of treated patients (*67*).

Recently, Kratochwil et al. reported on first-in-human PSMA-targeted α-therapy of metastatic prostate cancer with ^{225}Ac-labeled PSMA-617 (Fig. 4) (*68*). Strong antitumor activity and good tolerability were observed when ^{225}Ac-PSMA-617 was applied in 3 cycles at bimonthly intervals (*69*). The 6-mo follow-up revealed a better response in patients treated with ^{225}Ac-PSMA-617 than in patients

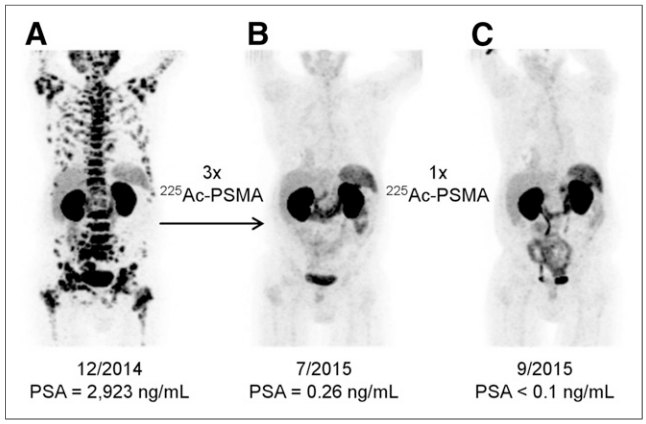

FIGURE 4. (A) ^{68}Ga-PSMA-11 PET/CT scan of patient with pretherapeutic tumor spread. PSA = prostate-specific antigen. (B) Restaging 2 mo after third cycle of ^{225}Ac-PSMA-617 (9–10 MBq). (C) Restaging 2 mo after single additional consolidation therapy (6 MBq). ^{177}Lu-PSMA-617 was contraindicated because of diffuse red marrow infiltration. (Reproduced from (*68*).)

treated with ^{177}Lu-PSMA-617; however, frequent and more severe xerostomia occurred (*70*). The impressive clinical results in highly challenging clinical situations demonstrated the effectiveness of the α-emitter (*68*).

BISMUTH-213

^{213}Bi is available from a ^{225}Ac/^{213}Bi generator (Table 1; Fig. 2). Successful α-therapy with ^{213}Bi has been demonstrated in many preclinical studies and several clinical trials (*52*). Clinically, ^{213}Bi-labeled substance P was used for local administration in patients with located gliomas (*71*). High retention of the activity at the target site and radiation-induced necrosis of tumors were observed, without relevant acute local or systemic toxicity (*71*). The application of ^{213}Bi-DOTATOC resulted in long-lasting antitumor responses in all treated patients (*72*). Despite the short physical half-life, even systemic application of ^{213}Bi-lintuzumab in 31 patients was effective and resulted in remissions in patients with acute myeloid leukemia (*73*).

CONCLUSION

Here we discussed several radionuclides with a high therapeutic potential because of their decay properties. For most of them, availability is limited and this factor affects cost negatively. Depending on demand from clinics, the cost can decrease if production takes place in the private sector. Future endeavors of physicists, radiochemists, and radiopharmacists should focus on the development of reliable and efficient production methods. The various physical decay properties, such as variable half-lives and the emission of high- and low-LET particles, could allow the application of the most appropriate radionuclide for a given cancerous disease. Given these features, systemic radionuclide therapy fits the concept of personalized medicine perfectly and, thus, is among the most modern therapeutic strategies to be pursued.

DISCLOSURE

No potential conflict of interest relevant to this article was reported.

REFERENCES

1. Zukotynski K, Jadvar H, Capala J, Fahey F. Targeted radionuclide therapy: practical applications and future prospects. *Biomark Cancer.* 2016;8:35–38.
2. Kam BL, Teunissen JJ, Krenning EP, et al. Lutetium-labelled peptides for therapy of neuroendocrine tumours. *Eur J Nucl Med Mol Imaging.* 2012;39 (suppl 1):S103–S112.
3. Kulkarni HR, Singh A, Schuchardt C, et al. PSMA-based radioligand therapy for metastatic castration-resistant prostate cancer: the Bad Berka experience since 2013. *J Nucl Med.* 2016;57(suppl):97S–104S.
4. Kassis AI. Therapeutic radionuclides: biophysical and radiobiologic principles. *Semin Nucl Med.* 2008;38:358–366.
5. Wissing MD, van Leeuwen FW, van der Pluijm G, Gelderblom H. Radium-223 chloride: extending life in prostate cancer patients by treating bone metastases. *Clin Cancer Res.* 2013;19:5822–5827.
6. Smith NA, Bowers DL, Ehst DA. The production, separation, and use of ^{67}Cu for radioimmunotherapy: a review. *Appl Radiat Isot.* 2012;70:2377–2383.
7. Mausner LF, Kolsky KL, Joshi V, Srivastava SC. Radionuclide development at BNL for nuclear medicine therapy. *Appl Radiat Isot.* 1998;49:285–294.
8. Wadas TJ, Wong EH, Weisman GR, Anderson CJ. Copper chelation chemistry and its role in copper radiopharmaceuticals. *Curr Pharm Des.* 2007;13:3–16.
9. Anderson CJ, Wadas TJ, Wong EH, Weisman GR. Cross-bridged macrocyclic chelators for stable complexation of copper radionuclides for PET imaging. *Q J Nucl Med Mol Imaging.* 2008;52:185–192.
10. Zimmermann K, Grünberg J, Honer M, Ametamey S, Schubiger PA, Novak-Hofer I. Targeting of renal carcinoma with $^{67/64}$Cu-labeled anti-L1-CAM antibody chCE7: selection of copper ligands and PET imaging. *Nucl Med Biol.* 2003;30:417–427.
11. Grünberg J, Novak-Hofer I, Honer M, et al. In vivo evaluation of ^{177}Lu- and $^{67/64}$Cu-labeled recombinant fragments of antibody chCE7 for radioimmunotherapy and PET imaging of L1-CAM-positive tumors. *Clin Cancer Res.* 2005;11:5112–5120.
12. Hughes OD, Bishop MC, Perkins AC, et al. Preclinical evaluation of copper-67 labelled anti-MUC1 mucin antibody C595 for therapeutic use in bladder cancer. *Eur J Nucl Med.* 1997;24:439–443.
13. Denardo GL, Denardo SJ, Kukis DL, et al. Maximum tolerated dose of ^{67}Cu-2IT-BAT-LYM-1 for fractionated radioimmunotherapy of non-Hodgkin's lymphoma: a pilot study. *Anticancer Res.* 1998;18:2779–2788.
14. DeNardo GL, Kukis DL, Shen S, DeNardo DA, Meares CF, DeNardo SJ. ^{67}Cu- versus ^{131}I-labeled Lym-1 antibody: comparative pharmacokinetics and dosimetry in patients with non-Hodgkin's lymphoma. *Clin Cancer Res.* 1999;5: 533–541.
15. O'Donnell RT, DeNardo GL, Kukis DL, et al. A clinical trial of radioimmunotherapy with ^{67}Cu-2IT-BAT-Lym-1 for non-Hodgkin's lymphoma. *J Nucl Med.* 1999;40:2014–2020.
16. Delaloye AB, Delaloye B, Buchegger F, et al. Comparison of copper-67- and iodine-125-labeled anti-CEA monoclonal antibody biodistribution in patients with colorectal tumors. *J Nucl Med.* 1997;38:847–853.
17. Müller C, Bunka M, Haller S, et al. Promising prospects for ^{44}Sc-/^{47}Sc-based theragnostics: application of ^{47}Sc for radionuclide tumor therapy in mice. *J Nucl Med.* 2014;55:1658–1664.
18. Bartos B, Majkowska A, Kasperek A, Krajewski S, Bilewicz A. New separation method of no-carrier-added ^{47}Sc from titanium targets. *Radiochim Acta.* 2012;100:457–461.
19. Srivastava SC. Paving the way to personalized medicine: production of some promising theragnostic radionuclides at Brookhaven National Laboratory. *Semin Nucl Med.* 2012;42:151–163.
20. Müller C, Bunka M, Reber J, et al. Promises of cyclotron-produced ^{44}Sc as a diagnostic match for trivalent β^--emitters: in vitro and in vivo study of a ^{44}Sc-DOTA-folate conjugate. *J Nucl Med.* 2013;54:2168–2174.
21. Rane S, Harris JT, Starovoitova VN. ^{47}Ca production for ^{47}Ca/^{47}Sc generator system using electron linacs. *Appl Radiat Isot.* 2015;97:188–192.
22. Price TW, Greenman J, Stasiuk GJ. Current advances in ligand design for inorganic positron emission tomography tracers ^{68}Ga, ^{64}Cu, ^{89}Zr and ^{44}Sc. *Dalton Trans.* 2016;45:15702–15724.
23. Kerdjoudj R, Pniok M, Alliot C, et al. Scandium(III) complexes of monophosphorus acid DOTA analogues: a thermodynamic and radiolabelling study with ^{44}Sc from cyclotron and from a ^{44}Ti/^{44}Sc generator. *Dalton Trans.* 2016;45: 1398–1409.
24. Nagy G, Szikra D, Trencsényi G, et al. AAZTA: an ideal chelating agent for the development of ^{44}Sc PET imaging agents. *Angew Chem Int Ed Engl.* 2017;56: 2118–2122.
25. Smits ML, Nijsen JF, van den Bosch MA, et al. Holmium-166 radioembolization for the treatment of patients with liver metastases: design of the phase I HEPAR trial. *J Exp Clin Cancer Res.* 2010;29:70.
26. Nijsen JF, Zonnenberg BA, Woittiez JR, et al. Holmium-166 poly lactic acid microspheres applicable for intra-arterial radionuclide therapy of hepatic malignancies: effects of preparation and neutron activation techniques. *Eur J Nucl Med.* 1999;26:699–704.
27. Nijsen F, Rook D, Brandt C, et al. Targeting of liver tumour in rats by selective delivery of holmium-166 loaded microspheres: a biodistribution study. *Eur J Nucl Med.* 2001;28:743–749.
28. Vente MA, Nijsen JF, de Wit TC, et al. Clinical effects of transcatheter hepatic arterial embolization with holmium-166 poly(L-lactic acid) microspheres in healthy pigs. *Eur J Nucl Med Mol Imaging.* 2008;35:1259–1271.
29. Prince JF, van Rooij R, Bol GH, de Jong HW, van den Bosch MA, Lam MG. Safety of a scout dose preceding hepatic radioembolization with ^{166}Ho microspheres. *J Nucl Med.* 2015;56:817–823.
30. Kim JK, Han KH, Lee JT, et al. Long-term clinical outcome of phase IIb clinical trial of percutaneous injection with holmium-166/chitosan complex (Milican) for the treatment of small hepatocellular carcinoma. *Clin Cancer Res.* 2006;12:543–548.
31. Dadachova E, Mirzadeh S, Lambrecht RM, Hetherington EL, Knapp FF. Separation of carrier-free holmium-166 from neutron-irradiated dysprosium targets. *Anal Chem.* 1994;66:4272–4277.
32. Li WP, Smith CJ, Cutler CS, Hoffman TJ, Ketring AR, Jurisson SS. Aminocarboxylate complexes and octreotide complexes with no carrier added ^{177}Lu, ^{166}Ho and ^{149}Pm. *Nucl Med Biol.* 2003;30:241–251.

33. Ueno NT, de Souza JA, Booser D, et al. Pilot study of targeted skeletal radiation therapy for bone-only metastatic breast cancer. *Clin Breast Cancer.* 2009;9:173–177.
34. Rajendran JG, Eary JF, Bensinger W, Durack LD, Vernon C, Fritzberg A. High-dose ^{166}Ho-DOTMP in myeloablative treatment of multiple myeloma: pharmacokinetics, biodistribution, and absorbed dose estimation. *J Nucl Med.* 2002;43:1383–1390.
35. Lehenberger S, Barkhausen C, Cohrs S, et al. The low-energy beta$^-$ and electron emitter ^{161}Tb as an alternative to ^{177}Lu for targeted radionuclide therapy. *Nucl Med Biol.* 2011;38:917–924.
36. Champion C, Quinto MA, Morgat C, Zanotti-Fregonara P, Hindie E. Comparison between three promising β-emitting radionuclides, ^{67}Cu, ^{47}Sc and ^{161}Tb, with emphasis on doses delivered to minimal residual disease. *Theranostics.* 2016;6:1611–1618.
37. Müller C, Zhernosekov K, Köster U, et al. A unique matched quadruplet of terbium radioisotopes for PET and SPECT and for α- and β$^-$-radionuclide therapy: an in vivo proof-of-concept study with a new receptor-targeted folate derivative. *J Nucl Med.* 2012;53:1951–1959.
38. Müller C, Reber J, Haller S, et al. Direct in vitro and in vivo comparison of ^{161}Tb and ^{177}Lu using a tumour-targeting folate conjugate. *Eur J Nucl Med Mol Imaging.* 2014;41:476–485.
39. Grünberg J, Lindenblatt D, Dorrer H, et al. Anti-L1CAM radioimmunotherapy is more effective with the radiolanthanide terbium-161 compared to lutetium-177 in an ovarian cancer model. *Eur J Nucl Med Mol Imaging.* 2014;41:1907–1915.
40. Haller S, Pellegrini G, Vermeulen C, et al. Contribution of Auger/conversion electrons to renal side effects after radionuclide therapy: preclinical comparison of ^{161}Tb-folate and ^{177}Lu-folate. *EJNMMI Res.* 2016;6:13.
41. Allen BJ, Blagojevic N. Alpha- and beta-emitting radiolanthanides in targeted cancer therapy: the potential role of terbium-149. *Nucl Med Commun.* 1996;17:40–47.
42. Beyer GJ, Comor JJ, Dakovic M, et al. Production routes of the alpha emitting ^{149}Tb for medical application. *Radiochim Acta.* 2002;90:247–252.
43. Beyer GJ, Miederer M, Vranjes-Durić S, et al. Targeted alpha therapy in vivo: direct evidence for single cancer cell kill using ^{149}Tb-rituximab. *Eur J Nucl Med Mol Imaging.* 2004;31:547–554.
44. Müller C, Reber J, Haller S, et al. Folate receptor targeted alpha-therapy using terbium-149. *Pharmaceuticals (Basel).* 2014;7:353–365.
45. Müller C, Vermeulen C, Köster U, et al. Alpha-PET with terbium-149: evidence and perspectives for radiotheragnostics [letter]. *EJNMMI Radiopharm Chem.* 2016;1:5.
46. Máthé D, Szigeti K, Hegedus N, et al. Production and in vivo imaging of ^{203}Pb as a surrogate isotope for in vivo ^{212}Pb internal absorbed dose studies. *Appl Radiat Isot.* 2016;114:1–6.
47. Atcher RW, Friedman AM, Hines JJ. An improved generator for the production of ^{212}Pb and ^{212}Bi from ^{224}Ra. *Int J Rad Appl Instrum A.* 1988;39:283–286.
48. Yong K, Brechbiel M. Application of ^{212}Pb for targeted α-particle therapy (TAT): pre-clinical and mechanistic understanding through to clinical translation. *AIMS Med Sci.* 2015;2:228–245.
49. Meredith RF, Torgue J, Azure MT, et al. Pharmacokinetics and imaging of ^{212}Pb-TCMC-trastuzumab after intraperitoneal administration in ovarian cancer patients. *Cancer Biother Radiopharm.* 2014;29:12–17.
50. Meredith R, Torgue J, Shen S, et al. Dose escalation and dosimetry of first-in-human α radioimmunotherapy with ^{212}Pb-TCMC-trastuzumab. *J Nucl Med.* 2014;55:1636–1642.
51. Elgqvist J, Frost S, Pouget J-P, Albertsson P. The potential and hurdles of targeted alpha therapy: clinical trials and beyond. *Front Oncol.* 2014;3:324.
52. Morgenstern A, Bruchertseifer F, Apostolidis C. Targeted alpha therapy with ^{213}Bi. *Curr Radiopharm.* 2011;4:295–305.
53. Apostolidis C, Molinet R, McGinley J, Abbas K, Mollenbeck J, Morgenstern A. Cyclotron production of Ac-225 for targeted alpha therapy. *Appl Radiat Isot.* 2005;62:383–387.
54. Boll RA, Malkemus D, Mirzadeh S. Production of actinium-225 for alpha particle mediated radioimmunotherapy. *Appl Radiat Isot.* 2005;62:667–679.
55. Weidner JW, Mashnik SG, John KD, et al. ^{225}Ac and ^{223}Ra production via 800 MeV proton irradiation of natural thorium targets. *Appl Radiat Isot.* 2012;70:2590–2595.
56. Zhuikov BL, Kalmykov SN, Ermolaev SV, et al. Production of ^{225}Ac and ^{223}Ra by irradiation of Th with accelerated protons. *Radiochemistry.* 2011;53:73–80.
57. Koch L, Apostolidis C, Janssens W, Molinet R, Van Geel J. Production of Ac-225 and application of the Bi-213 daughter in cancer therapy. *Czechoslovak J Phys.* 1999;49(suppl 1):817–822.
58. Melville G, Allen BJ. Cyclotron and linac production of Ac-225. *Appl Radiat Isot.* 2009;67:549–555.
59. de Kruijff RM, Wolterbeek HT, Denkova AG. A critical review of alpha radionuclide therapy: how to deal with recoiling daughters? *Pharmaceuticals (Basel).* 2015;8:321–336.
60. Miederer M, McDevitt MR, Sgouros G, Kramer K, Cheung NK, Scheinberg DA. Pharmacokinetics, dosimetry, and toxicity of the targetable atomic generator, ^{225}Ac-HuM195, in nonhuman primates. *J Nucl Med.* 2004;45:129–137.
61. Aghevlian S, Boyle AJ, Reilly RM. Radioimmunotherapy of cancer with high linear energy transfer (LET) radiation delivered by radionuclides emitting α-particles or Auger electrons. *Adv Drug Deliv Rev.* 2017;109:102–118.
62. Wadas TJ, Pandya DN, Solingapuram Sai KK, Mintz A. Molecular targeted alpha-particle therapy for oncologic applications. *AJR.* 2014;203:253–260.
63. McDevitt MR, Ma D, Lai LT, et al. Tumor therapy with targeted atomic nanogenerators. *Science.* 2001;294:1537–1540.
64. Miederer M, Henriksen G, Alke A, et al. Preclinical evaluation of the alpha-particle generator nuclide ^{225}Ac for somatostatin receptor radiotherapy of neuroendocrine tumors. *Clin Cancer Res.* 2008;14:3555–3561.
65. Borchardt PE, Yuan RR, Miederer M, McDevitt MR, Scheinberg DA. Targeted actinium-225 in vivo generators for therapy of ovarian cancer. *Cancer Res.* 2003;63:5084–5090.
66. Jurcic JG, Rosenblat TL, McDevitt MR, et al. Phase I trial of the targeted alpha-particle nano-generator actinium-225 (^{225}Ac-lintuzumab) (anti-CD33; HuM195) in acute myeloid leukemia (AML) [abstract]. *J Clin Oncol.* 2011;29(suppl):6516.
67. Franz B, Rosenblat TL, McDevitt MR, et al. Phase I trial of the targeted alpha-particle nano-generator actinium-225 (Ac-225)-lintuzumab (anti-CD33; HuM195) in acute myeloid leukemia (AML). *Blood.* 2011;118:348–357.
68. Kratochwil C, Bruchertseifer F, Giesel FL, et al. ^{225}Ac-PSMA-617 for PSMA-targeted alpha-radiation therapy of metastatic castration-resistant prostate cancer. *J Nucl Med.* 2016;57:1941–1944.
69. Kratochwil C, Bruchertseifer F, Giesel F, Apostolidis C, Haberkorn U, Morgenstern A. Dose escalation experience with ^{225}Ac-PSMA-617 in PSMA targeting alpha-radiation therapy of patients with mCRPC. *Eur J Nucl Med Mol Imaging.* 2016;43(suppl 1):S51.
70. Kratochwil C, Bruchertseifer F, Giesel F, Apostolidis C, Haberkorn U, Morgenstern A. ^{225}Ac-PSMA-617 for PSMA targeting alpha-radiation therapy of 28 patients with mCRPC. *Eur J Nucl Med Mol Imaging.* 2016;43(suppl 1):S137.
71. Cordier D, Forrer F, Bruchertseifer F, et al. Targeted alpha-radionuclide therapy of functionally critically located gliomas with ^{213}Bi-DOTA-[Thi^8,Met$(O_2)^{11}$]-substance P: a pilot trial. *Eur J Nucl Med Mol Imaging.* 2010;37:1335–1344.
72. Kratochwil C, Giesel FL, Bruchertseifer F, et al. ^{213}Bi-DOTATOC receptor-targeted alpha-radionuclide therapy induces remission in neuroendocrine tumours refractory to beta radiation: a first-in-human experience. *Eur J Nucl Med Mol Imaging.* 2014;41:2106–2119.
73. Rosenblat TL, McDevitt MR, Mulford DA, et al. Sequential cytarabine and alpha-particle immunotherapy with bismuth-213-lintuzumab (HuM195) for acute myeloid leukemia. *Clin Cancer Res.* 2010;16:5303–5311.
74. Pillai MR, Chakraborty S, Das T, Venkatesh M, Ramamoorthy N. Production logistics of ^{177}Lu for radionuclide therapy. *Appl Radiat Isot.* 2003;59:109–118.
75. Lebedev NA, Novgorodov AF, Misiak R, Brockmann J, Rösch F. Radiochemical separation of no-carrier-added ^{177}Lu as produced via the ^{176}Yb(n,γ)^{177}Yb→^{177}Lu process. *Appl Radiat Isot.* 2000;53:421–425.
76. Yagi M, Kondo K. Preparation of carrier-free ^{67}Cu by the ^{68}Zn(γ,p) reaction. *Int J Appl Radiat Isot.* 1978;29:757–759.
77. Mirzadeh S, Mausner LF, Srivastava SC. Production of no-carrier added ^{67}Cu. *Int J Rad Appl Instrum A.* 1986;37:29–36.
78. Kozempel J, Abbas K, Simonelli F, Bulgheroni A, Holzwarth U, Gibson N. Preparation of ^{67}Cu via deuteron irradiation of ^{70}Zn. *Radiochim Acta.* 2012;100:419–423.